Reversible Adduct Formation of Trimethylgallium and Trimethylindium with Ammonia

J. Randall Creighton* and George T. Wang

Sandia National Laboratories, P.O. Box 5800, MS-0601, Albuquerque, New Mexico 87185

Received: August 4, 2004; In Final Form: October 19, 2004

We have used gas-phase infrared spectroscopy to determine the equilibrium constant (K_p) for the formation of $(CH_3)_3Ga{:}NH_3$ and $(CH_3)_3In{:}NH_3$ adducts in the 80−230 °C range. In this temperature range, and at reactant concentrations typically used for metal organic chemical vapor deposition, the dominant chemical reaction is reversible adduct formation/dissociation. Reaction enthalpies and entropies are extracted from the temperature dependence of K_p, yielding $\Delta H(\mathrm{Ga}) = -16.3 \pm 0.5$ kcal/mol, $\Delta S(\mathrm{Ga}) = -32.4 \pm 1.2$ eu, and $\Delta H(\mathrm{In}) = -15.0 \pm 0.6$ kcal/mol, $\Delta S(\mathrm{In}) = -30.3 \pm 1.4$ eu. These results will aid current and future modeling efforts, as well as advance our general understanding of the group-III nitride deposition process.

1. Introduction

Gallium nitride and AlGaInN alloy semiconductors are in widespread use for a variety of optoelectronic and electronic applications.[1] Metal organic chemical vapor deposition (MOCVD) is the dominant method of depositing AlGaInN films, which are typically grown in the 700−1100 °C temperature range. Unfortunately, the high temperatures required to deposit high-quality material can also lead to the initiation of parasitic gas-phase chemical reactions.[2−7] These parasitic chemical reactions have a number of deleterious consequences that generally make it much harder to control and reproduce the MOCVD process.

We previously reported that the parasitic chemical reactions during AlGaInN MOCVD lead to the formation of gas-phase nanoparticles,[8−9] which are suspended away from the growing film by a thermophoretic force. These nanoparticles represent the end product of a sequence of gas-phase nucleation and particle growth reactions that are still not well understood. Any attempt to understand the parasitic chemical mechanism must at some point deal with possible adduct formation reactions between NH_3 and trimethylgallium (TMGa), or trimethylaluminum (TMAl), or trimethylindium (TMIn), as in reaction 1.

$$M(CH_3)_3 + NH_3 \leftrightarrow (CH_3)_3M{:}NH_3 \quad M = \mathrm{Al, Ga, In} \qquad (1)$$

Formation of the group-III/ammonia adduct, $(CH_3)_3M{:}NH_3$, appears inevitable at the point where the gases are mixed in any conventional MOCVD system. Whether or not this reaction represents the first step in the parasitic chemical reaction mechanism is still somewhat controversial and may depend on which group-III element is involved. One pathway often proposed involves a CH_4 elimination reaction from the adduct, forming the $(CH_3)_2M-NH_2$ species.[10,11] Further CH_4 elimination and oligomerization could initiate particle nucleation. We have recently shown that at ∼250 °C the $TMAl{:}NH_3$ adduct is completely converted into gas-phase $(CH_3)_2AlNH_2$ at nominal MOCVD concentrations and residence times.[9] Therefore, adduct formation and elimination reactions may play an important role in the early stages of the overall parasitic reaction mechanism when growing AlN or Al-containing alloys.

Whether or not a similar pathway at MOCVD conditions is active for TMGa and TMIn is more debatable. Some early experimental work implied that the analogous pathway for TMGa is viable,[11] but theoretical investigations[12] and more recent experimental work[9,13] have questioned the importance of this pathway. In a recent publication, we used Fourier transform infrared spectroscopy (FTIR) to examine the initial reactivity of gas-phase ammonia with TMAl, TMGa, and TMIn, from room temperature up to ∼300 °C, at nominal reactor concentrations and residence times.[9] The irreversible reaction of the $TMAl{:}NH_3$ adduct was easily observable, with CH_4 being detected near 120 °C and formed quantitatively at 250 °C. However, evidence for the analogous pathway for $TMGa{:}NH_3$ and $TMIn{:}NH_3$ was not seen (no CH_4 detected) below 280 °C. Instead, reversible adduct formation/dissociation was the dominant chemical reaction for TMGa (TMIn) + NH_3 mixtures. In this paper, we analyze FTIR spectra in the 80−230 °C range to determine the equilibrium constant (K_p) for the $TMGa{:}NH_3$ and $TMIn{:}NH_3$ adducts. Reaction enthalpies and entropies are extracted from the temperature dependence of K_p and are compared to available theoretical and experimental results.

2. Experimental Procedure

Gas-phase infrared spectroscopy was performed with a Mattson RS-1 FTIR spectrometer. A heatable long path length gas cell was mounted in the sample compartment of the instrument (see Figure 1). The IR beam enters and exits through a single KCl window (6 mm thickness) and is folded once with a Au-coated spherical mirror ($r = 40.6$ cm), giving an internal path length of ∼80 cm. This intermediate value of path length was chosen as a compromise to yield a reasonable absorbance for the organometallic precursors and adducts without yielding an excessive absorbance from the gas-phase NH_3 (which is ∼500× higher in concentration). The cell was contained in an Al-lined furnace and could be heated to ∼300 °C. This upper temperature limit is determined by the thermal properties of the fluorocarbon-based elastomeric O-ring used on the KCl window seal. Gas temperature was monitored with three internal (top-center-bottom) type-K thermocouples, and the maximum temperature gradient was typically ≤2 °C. Spectra were collected at 2 cm^{-1} resolution from 450 to 4000 cm^{-1}. At the

* Corresponding author. E-mail: jrcreig@sandia.gov.

10.1021/jp046491h CCC: $30.25
Published on Web 12/08/2004

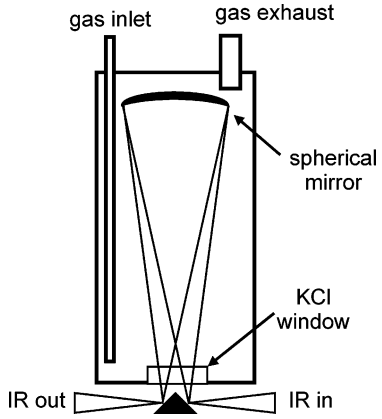

Figure 1. Schematic of the double-pass FTIR gas cell.

higher cell temperatures, the increased absorption by the KCl window limited the lower effective wavenumber to ~500 cm^{-1}.

The gas cell was connected in parallel with our research MOCVD reactor and operated at flow rates and pressures in the same nominal range used for AlGaInN deposition. Gases were mixed before injection into the cell, with concentrations kept below the onset of adduct condensation.[14] The long internal gas inlet tube allowed the gases to preheat before they were fully introduced into the cell.

The total pressure was varied from 50 to 200 Torr, with a total flow rate of 6.5 slm. For this flow rate, at 300 K and 100 Torr total pressure, the mean residence time in the cell is 3.5 s (internal volume = 3.2 L). Hydrogen was used as the carrier gas. The ammonia flow rate was fixed at 1.0 slm, giving $P(NH_3)$ = 15.4 Torr at the 100 Torr total pressure condition. TMGa and TMIn were delivered using a standard bubbler configuration to give P(TMGa) = 62.8 mTorr and P(TMIn) = 20.3 mTorr at the 100 Torr total pressure condition. The partial pressure of the reactants scales with total pressure, so at 200 Torr the values are double the 100 Torr values given above. We note that there is considerable uncertainty in the TMIn vapor pressure[15] and bubbler efficiency, but errors in the metal organic partial pressure tend to cancel out in the determination of the equilibrium constant (see section 3.3). The detection limit for CH_4 at the 100 Torr total pressure condition is 0.3 mTorr, and no CH_4 was detected in the temperature range used to determine the equilibrium constants.

An example of the IR spectrum for a TMGa + NH_3 + H_2 mixture (using pure H_2 as the reference spectrum) is shown in Figure 2, curve a. The spectrum is dominated by the strong NH_3(g) absorption, which obscures most of the peaks due to TMGa:NH_3 and/or free TMGa. The NH_3 absorption is removed by using a reference spectrum of a NH_3 + H_2 mixture at the same pressure and temperature, revealing a large number of modes that can be assigned to the TMGa:NH_3 adduct (see Figure 2, curve b). Because of strong NH_3(g) IR absorption, small concentration differences between the sample and reference spectra, and/or slight inaccuracies in the FTIR data acquisition procedure, sometimes led to small residual NH_3-derived features on the baseline. These artifacts are most often seen at 3335, 1626, 964, and 930 cm^{-1} and are denoted with asterisks.

3. Results and Discussion

3.1. Infrared Spectroscopy of $Ga(CH_3)_3$ + NH_3 Mixtures. Near room temperature and for the reactant partial pressures studied, the TMGa:NH_3 adduct is formed and is nearly 100% associated. A number of unique modes appear in the TMGa:NH_3 FTIR spectrum (see Figure 3, curve a) that are not

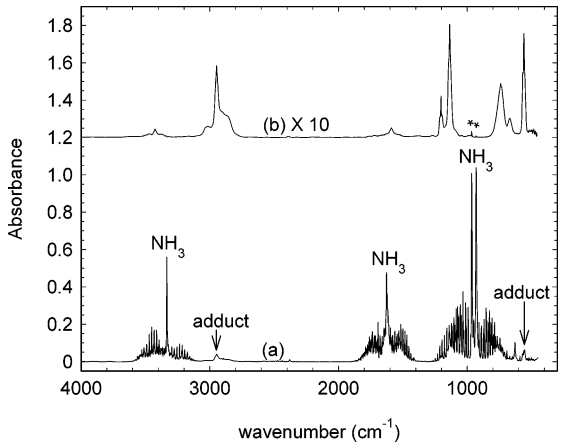

Figure 2. FTIR of a TMGa + NH_3 mixture at 23 °C, $P(NH_3)$ = 15.4 Torr, P(TMGa) = 62.8 mTorr, P_{total} = 100 Torr. Curve a uses a pure H_2 reference spectrum, and both NH_3(g) and adduct modes are visible. Curve b uses a H_2 + NH_3 reference spectrum so only adduct modes are visible. Asterisks (*) denote small residual NH_3 artifacts in curve b.

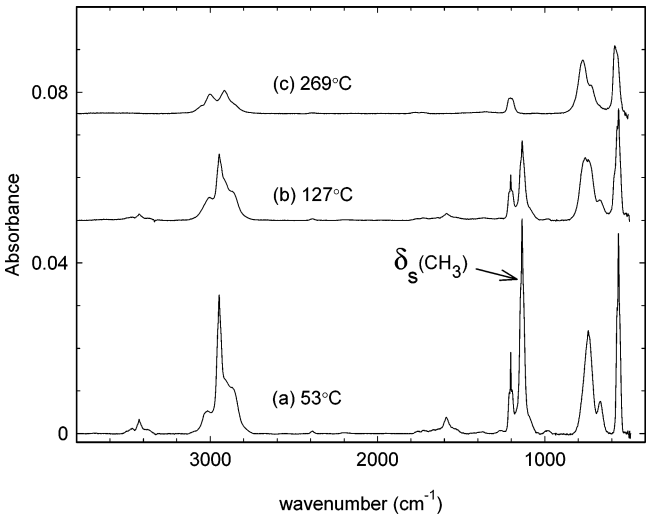

Figure 3. FTIR of TMGa + NH_3 mixtures at 100 Torr total pressure for temperatures of (a) 53, (b) 127, and (c) 269 °C. Partial pressures are $P(NH_3)$ = 15.4 Torr, P(TMGa) = 62.8 mTorr. NH_3 absorption has been removed and curves have been offset for clarity.

attributed to TMGa(g) or NH_3(g). This spectrum is in good agreement with other reports[16−18] and is discussed in more detail in a previous publication.[9] The most intense TMGa:NH_3 peak that does not significantly overlap with any TMGa feature is at 1136 cm^{-1} and has been assigned as a $\delta_s(CH_3)$ mode. The δ_s-(CH_3) mode for TMGa:NH_3 is shifted significantly from the corresponding mode in pure TMGa (near 1200 cm^{-1}), so it serves as a good indicator of the amount of adduct present. Upon heating above ~100 °C, the equilibrium (reaction 1) begins to shift back to free TMGa(g) and NH_3(g) and the peaks corresponding to the adduct begin to diminish. At 127 °C (Figure 3, curve b), the integrated intensity of the $\delta_s(CH_3)$ mode indicates that roughly 40% of the adduct is dissociated. The spectrum of the mixture at this temperature is composed entirely of free TMGa(g) and the adduct, with no CH_4(g) or other species detected. At 269 °C (Figure 3, curve c), the adduct modes are not detectable and the spectrum is identical to pure TMGa(g), indicating nearly 100% dissociation (~0% association).

3.2. Infrared Spectroscopy of $In(CH_3)_3$ + NH_3 Mixtures. The reaction of TMIn with NH_3 has not been studied in as much detail as the corresponding TMAl or TMGa chemistry. Besides

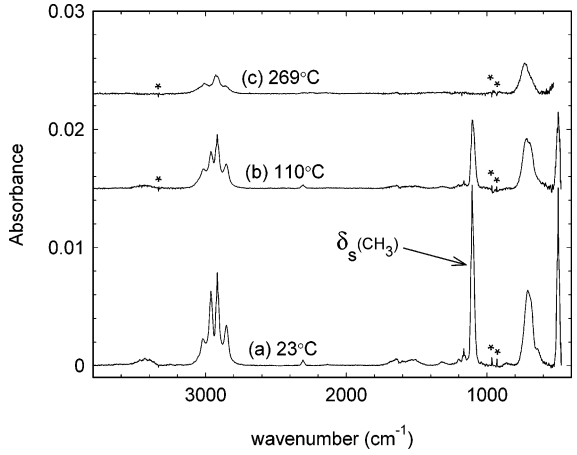

Figure 4. FTIR of TMIn + NH_3 mixtures at 100 Torr total pressure for temperatures of (a) 23, (b) 110, and (c) 269 °C. Partial pressures are $P(NH_3) = 15.4$ Torr, P(TMIn) = 20.3 mTorr. NH_3 absorption has been removed and curves have been offset for clarity.

our work, only one other IR study has been reported,[19] in this case for matrix-isolated (condensed-phase) TMIn:NH_3. Our spectrum for the gas-phase TMIn:NH_3 adduct is shown in Figure 4, curve a. Many qualitative similarities between the TMIn:NH_3 and TMGa:NH_3 adduct are apparent. On the basis of similarities with the TMGa:NH_3, we previously assigned the intense peak at 1106 cm^{-1} seen for TMIn:NH_3 to the $\delta_s(CH_3)$ mode.[9] This peak is also a good indicator of the amount of TMIn:NH_3 present because it does not significantly overlap with any TMIn modes.

As the TMIn + NH_3 mixture is heated to ~100 °C, simple adduct dissociation occurs, analogous to the case for TMGa:NH_3. The spectrum of a TMIn + NH_3 mixture at 110 °C is shown in Figure 4, curve b, and the intensity of the $\delta_s(CH_3)$ adduct mode indicates ~40% dissociation. Spectra in the 100−200 °C range appear as linear combinations of TMIn:NH_3 and TMIn, and no CH_4 or other species are detected. At 269 °C, the spectrum of the mixture (Figure 4, curve c) is identical to pure TMIn, indicating nearly 100% dissociation of the TMIn:NH_3 adduct.

3.3. Determination of the Equilibrium Constant (K_p). The infrared spectra of the TMGa (TMIn) mixtures allow us to calculate the degree of association (α), see eq 2, where P(adduct) = adduct partial pressure, $P(MO)^0$ = initial TMGa or TMIn partial pressure. From the degree of association, we can determine the equilibrium constant (K_p), see eq 3. The expression in eq 3 is simplified because the NH_3 partial pressure (in great excess) is not affected by the degree of association.

$$\alpha = P(\text{adduct})/P(\text{MO})^0 \quad (2)$$

$$K_p = (P(\text{adduct})/P(\text{MO})P(NH_3)) = (\alpha/(1-\alpha)P(NH_3)) \quad (3)$$

In practice, α is determined from the ratio of the integrated absorbance of the $\delta_s(CH_3)$ adduct mode to its integrated absorbance near room temperature, after accounting for ideal gas expansion. Results for TMGa:NH_3 are shown in Figure 5, and results for TMIn:NH_3 are in Figure 6, as a function of temperature and total pressure (partial pressures scale with total pressure in these experiments). Generally, α begins to fall at temperatures above 100 °C, with the TMIn:NH_3 adduct being somewhat less stable than the TMGa:NH_3 adduct. As expected, increasing the NH_3 partial pressure causes α to increase, as the equilibrium (1) is shifted back toward adduct formation. The solid lines in Figures 5 and 6 are generated using the equilibrium

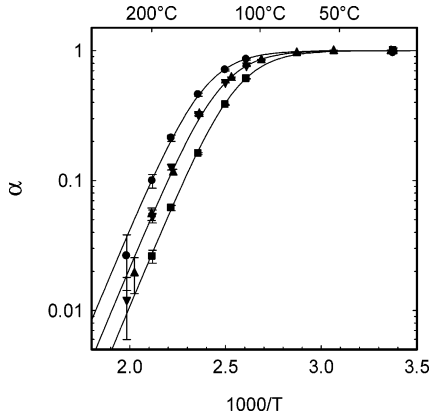

Figure 5. Temperature dependence of the degree of association (α) of TMGa + NH_3 mixtures at: $P = 50$ (■), 100 (▲), and 200 (●) Torr. Solid curves are generated from eq 3.

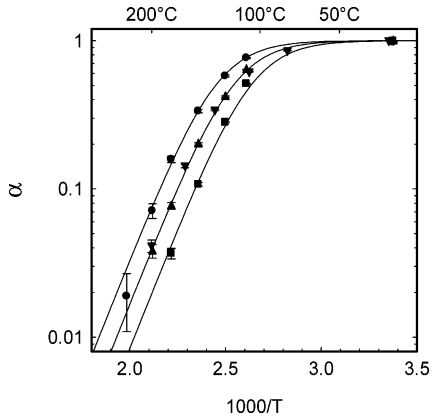

Figure 6. Temperature dependence of the degree of association (α) of TMIn + NH_3 mixtures at: $P = 50$ (■), 100 (▲), and 200 (●) Torr. Solid curves are generated from eq 3.

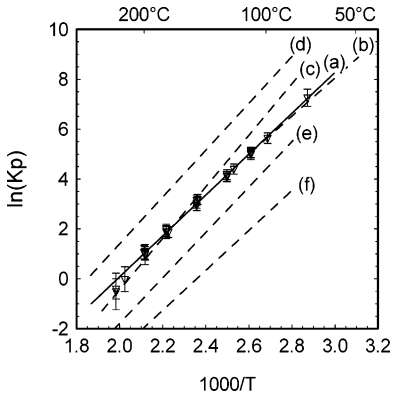

Figure 7. Equilibrium constant for TMGa:NH_3 mixtures, triangles represent experimental data; best fit, curve a; experimental value, ref 20, curve b; ref 22, curve c; ref 21, curve d; ref 23, curve e; theoretical value, ref 20, curve f.

constants derived from this analysis (vide infra), and they reproduce the observed temperature and pressure dependence extremely well.

After obtaining α, it is a simple matter to calculate K_p, and the results for TMGa:NH_3 and TMIn:NH_3 are shown in Figures 7 and 8, respectively. Measurements of α at differing pressures generate a common K_p, as expected. The enthalpy and entropy change for reaction 1 can be extracted from the temperature dependence of K_p. For TMGa:NH_3, the best fit (weighted least squares, 24 points) yields $\Delta H = -16.3 \pm 0.5$ kcal/mol and $\Delta S = -32.4 \pm 1.2$ eu. Comparison of these values to a variety of

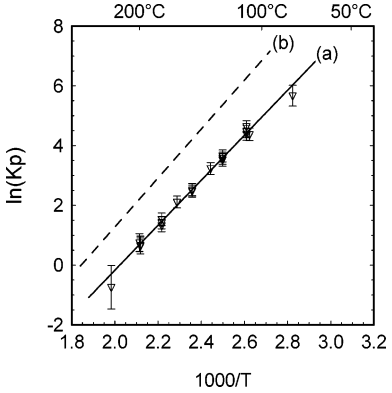

Figure 8. Equilibrium constant for TMIn:NH_3, triangles represent experimental data; best fit, curve a; theoretical value from ref 26, curve b.

TABLE 1: Thermodynamic Values for the TMGa:NH_3 Association Reaction

ref	ΔH (kcal/mol)	ΔS (eu)	K_p (atm^{-1}) at 100 °C
this work (experiment)	−16.3	−32.4	2.84×10^2
20 (experiment)	−15.2	−29.6	2.71×10^2
20 (theory)	−15.9	−37.5	1.31×10^1
21 (experiment)	−18.6	−34.5	2.39×10^3
22 (theory)	−20.5	−41.9	7.18×10^2
23 (theory)	−18.1	−39.7	8.15×10^1
24 (theory)	−18	−41	3.8×10^1
25 (theory)	−16.2	not given	not applicable

TABLE 2: Thermodynamic Values for the TMIn:NH_3 Association Reaction

ref	ΔH (kcal/mol)	ΔS (eu)	K_p (atm^{-1}) at 100 °C
this work (exp)	−15.0	−30.3	1.41×10^2
26 (theory)	−16.0	−29.2	1.02×10^3
25 (theory)	−16.1	not given	not applicable

experimental and theoretical measurements is shown in Figure 7 and Table 1. The only other direct experimental measurement of K_p was by Pelekh and Carr,[20] who used a total pressure measurement method for equimolar NH_3−TMGa mixtures between 40 and 100 °C (Figure 7, curve b). In the range of overlap, our measurements agree within experimental uncertainties (at 100 °C, they agree within 5%, see Table 1). Values of ΔH and ΔS from Pelekh and Carr[20] are both slightly smaller in magnitude than our measurement, but the agreement is within experimental uncertainties.

Przhevalskii et al.[21] used an indirect experimental estimate for the enthalpy ($\Delta H = -18.6$ kcal/mol) and derived the entropy change from a variety of experimental sources. Their overestimation of ΔH leads to an equilibrium constant that is about 8× too large (Figure 7, curve d) at 100 °C. The theoretical values of ΔH range from −15.9 to −20.5 kcal/mol, and values of ΔS range from −37.5 to − 41.9 eu.[20,22−25] Some of the theoretical values for ΔH are in good agreement with the experimental values (this work and ref 20), but ΔS is consistently overestimated (in magnitude), which generally leads to an underestimation of K_p.

For TMIn:NH_3, the best fit (weighted least squares, 20 points) from the K_p data yields $\Delta H = -15.0 \pm 0.6$ kcal/mol and $\Delta S = -30.3 \pm 1.4$ eu (Figure 8, curve a). For the TMIn adduct, there are much fewer theoretical studies and no experimental studies with which to compare our results. The two theoretical values for ΔH are slightly more negative than our result (see Table 2), but the agreement should be considered good. The theoretical value for ΔS from Cardelino et al.[26] is also in good agreement with our result, but the resulting value for K_p is about 7× too large (Figure 8, curve b) at 100 °C.

Finally, we note the similarity in the TMGa:NH_3 and TMIn:NH_3 results. The formation of the TMGa adduct is slightly more energetically favorable (by 1.3 kcal/mol) than the TMIn adduct. If the entropy change for each adduct were the same, then K_p for the TMGa adduct would be ∼6× larger than the TMIn adduct (at 100 °C). However, ΔS for the TMGa adduct is more negative than the TMIn adduct, resulting in K_p(Ga) being only 2× larger than K_p(In). In fact, at temperatures >500 °C, our results imply that K_p(In) will become larger than K_p(Ga).

4. Summary

In the 20−270 °C temperature range, reversible adduct formation−dissociation is the dominant reaction observed by FTIR for TMGa + NH_3 and TMIn + NH_3 mixtures, at concentrations typical of GaN and InGaN MOCVD inlet conditions. Using the FTIR spectra, the equilibrium constant (K_p) for the two adducts was determined in the 80−230 °C range. Results for K_p(Ga) are in excellent quantitative agreement with values from Pelekh and Carr[20] near 100 °C (where the two experimental methods overlap). Reaction enthalpies and entropies are extracted from the temperature dependence of K_p, yielding ΔH(Ga) = −16.3 ± 0.5 kcal/mol, ΔS(Ga) = −32.4 ± 1.2 eu, and ΔH(In) = −15.0 ± 0.6 kcal/mol, ΔS(In) = −30.3 ± 1.4 eu. The observed reaction enthalpy of the TMGa:NH_3 adduct is in good agreement with the value from Pelekh and Carr[20] and some of the more recent theoretical calculations.[20,25] For the TMGa:NH_3 adduct, the quantum chemical calculations tend to calculate a ΔS that is more negative than we observe, which causes the theoretical values for K_p(Ga) to be underestimated by about 1 order of magnitude. Much less literature exists for the TMIn:NH_3 adduct, but the experimentally observed reaction enthalpy and entropy of the TMIn:NH_3 adduct are in good agreement with recent theoretical calculations. Although the TMGa:NH_3 adduct has a larger reaction enthalpy than the TMIn:NH_3 adduct (as expected), net values for K_p(Ga) and K_p(In) are relatively close, being within a factor of 2 over the range measured. These results will aid current and future modeling efforts, as well as advance our general understanding of the group-III nitride MOCVD process.

Acknowledgment. We thank Dan Koleske for a critical reading of this manuscript, and T.M. Kerley and M. J. Russell for technical assistance. Sandia is a multiprogram laboratory operated by Sandia Corp., a Lockheed Martin Co. for the United States Department of Energy's National Nuclear Security Administration under contract No. DE-AC04-94AL85000. We especially acknowledge support from the Office of Basic Energy Sciences.

References and Notes

(1) Pankove, J. I.; Moustakas, T. D. *Gallium nitride (GaN) II. Semiconductors and semimetals*; Academic Press: San Diego, CA, 1999; Vol. 57 and references therein.

(2) Han, J.; Figiel, J. J.; Crawford, M. H.; Banas, M. A.; Bartram, M. E.; Biefeld, R. M.; Song, Y. K.; Nurmikko, A. V. *J. Cryst. Growth* **1998**, *195*, 291.

(3) Chen, C. H.; Liu, H.; Steigerwald, D.; Imler, W.; Kuo, C. P.; Craford, M. G.; Ludowise, M.; Lester, S.; Amano, J. *J. Electron. Mater.* **1996**, *25*, 1004.

(4) Sayyah, K.; Chung, B.-C.; Gershenzon, M. *J. Cryst. Growth* **1986**, *77*, 424.

(5) Nakamura, F.; Hashimoto, S.; Hara, M.; Imanaga, S.; Ikeda, M.; Kawai, H. *J. Cryst. Growth* **1998**, *195*, 280.

(6) Safvi, S. A.; Redwing, J. M.; Tischler, M. A.; Kuech, T. F. *J. Electrochem. Soc.* **1997**, *144*, 1789.
(7) Creighton, J. R.; Coltrin, M. E.; Breiland, W. G. *ECS Proc.* **2002**−**2003**, 28−35.
(8) Creighton, J. R.; Breiland, W. G.; Coltrin, M. E.; Pawlowski R. P. *Appl. Phys. Lett.* **2002**, *81*, 2626.
(9) Creighton, J. R.; Wang, G. T.; Breiland, W. G.; Coltrin, M. E. *J. Cryst. Growth* **2004**, *261*, 204.
(10) Mihopoulos, T. G.; Gupta, V.; Jensen, K. F. *J. Cryst. Growth* **1998**, *195*, 733.
(11) Thon, A.; Kuech, T. F. *Appl. Phys. Lett.* **1996**, *69*, 55.
(12) Sengupta, D. *J. Phys. Chem. B* **2003**, *107*, 291.
(13) Schäfer, J.; Simmons, A.; Wolfrum, J.; Fischer, R. A. *Chem. Phys. Lett.* **2000**, *319*, 477.
(14) Creighton, J. R. *J. Electron. Mater.* **2002**, *31*, 1337.
(15) Shenai, D. V.; Timmons, M. L.; DiCarlo, R. L.; Lemnah, G. K.; Stennick, R. S. *J. Cryst. Growth* **2003**, *248*, 91.
(16) Sywe, B. S.; Schlup, J. R.; Edgar, J. H. *Chem. Mater.* **1991**, *3*, 737.
(17) Almond, M. J.; Jenkins, C. E.; Rice, D. A.; Hagen, K. *J. Organomet. Chem.* **1992**, *439*, 251.
(18) Kim, S. H.; Kim, H. S.; Hwang, J. S.; Choi, J. G.; Chong, P. J. *Chem. Mater.* **1994**, *6*, 278.
(19) Piocos, E. A.; Ault, B. S. *J. Mol. Struct.* **1999**, *476*, 283.
(20) Pelekh, A.; Carr, R. W. *J. Phys. Chem. A* **2001**, *105*, 4697.
(21) Przhevalskii, I. N.; Karpov, S. Y.; Makarov, Y. N. *MRS Internet J. Nitride Semicond. Res.* **1998**, *3*, 30.
(22) Simka, H.; Willis, B. G.; Lengyel, I.; Jensen, K. F. *Prog. Cryst. Growth Charact.* **1997**, *2*−*4*, 117.
(23) Timoshkin, A. Y.; Bettinger, H. F.; Schaefer, H. F., III *J. Phys. Chem.* **2001**, *105*, 3240.
(24) Watwe, R. M.; Dumesic, J. A.; Kuech, T. F. *J. Cryst. Growth* **2000**, *221*, 751.
(25) Ikenaga, M.; Nakamura, K.; Tachibana, A.; Matsumoto, K. *J. Cryst. Growth* **2002**, *237*−*239*, 936.
(26) Cardelino, B. H.; Moore, C. E.; Cardelino, C. A.; Frazier, D. O.; Bachmann, K. J. *J. Phys. Chem. A* **2001**, *105*, 849.